Journal of the Taiwan Institute of Chemical Engineers 153 (2023) 105214

Contents lists available at ScienceDirect

Journal of the Taiwan Institute of Chemical Engineers

journal homepage: www.journals.elsevier.com/journal-of-the-taiwan-institute-of-chemical-engineers

Effect of polyhedral oligomeric silsesquioxane (POSS) nanoparticle on the miscibility and hydrogen bonding behavior of CO_2 based poly(cyclohexene carbonate) copolymers

Yen-Ling Kuan [a], Wei-Ting Du [a], Shiao-Wei Kuo [a,b,*]

[a] Department of Materials and Optoelectronic Science, Center for Functional Polymers and Supramolecular Materials, National Sun Yat-Sen University, Kaohsiung 80424, Taiwan
[b] Department of Medicinal and Applied Chemistry, Kaohsiung Medical University, Kaohsiung 80708, Taiwan

ARTICLE INFO

Keywords:
Polycarbonate
CO_2
Polyhedral oligomeric silsesquioxane
Screening effect
Hydrogen bonding interactions

ABSTRACT

Background: Since the Industrial Revolution in the 1890s, cities have grown exponentially, leading to a significant increase in carbon dioxide emissions and contributing to a growing global environmental crisis. Carbon dioxide capture and storage alone cannot fully address the issue of carbon cycle imbalance. One promising approach is to convert carbon dioxide into polycarbonate polymer, which possesses good biodegradability and is considered a viable alternative to petroleum-based polyester.

Methods: In this experiment, poly(cyclohexene carbonate) copolymer containing polyhedral oligomeric sesquioxane (PCHCPOSS) was prepared using ring-opening copolymerization (ROCOP) method. By mixing it with poly(vinyl phenol) (PVPh), we can observe the forces both intramolecular and intermolecular hydrogen bonding interaction.

Significant Findings: The binary blend of PVPh/PCHCPOSS10 exhibits a single T_g value throughout the composition, indicating complete miscibility. When the proportion of POSS increases, these blends show two different T_g values, suggesting that the addition of POSS does not promote miscibility. The FTIR results indicate that POSS reduces the formation of intermolecular hydrogen bonding interaction. This is attributed to the screening effect in the PVPh/PCHCPOSS binary blend, which significantly diminishes the formation of hydrogen bonds between OH and O=C.

1. Introduction

Global warming stands as a foremost concern among citizens, and the alternation of climate is primarily driven by greenhouse gas emissions currently. Carbon dioxide (CO_2) constitutes over 80 % of the total emissions of greenhouse gasses (GHGs) and garners much attention as the primary contributor. Most of the CO_2 comes from industrial production and the use of fossil fuels. Consequently, substantial research is directly towards the feasibility of CO_2 capture, storage or conversion into materials such as graphene, carbon nanotubes and nanofibers to achieve carbon neutrality [1–13]. Remarkably, CO_2 is not only nontoxic and abundant renewable resource, but also economically viable and easily accessible in large quantities [2,14]. However, a key concern pertains to the biodegradability of plastics, which typically did not degrade naturally, and thus to enhance the degradability of plastics could significantly mitigate environmental harm [15,16].

The utilization of CO_2 as a monomer exhibited the potential to enable large-scale synthesis of completely biodegradable copolymers, encompassing polycarbonates and their possible corresponding counterparts. Pioneers in this field, Inoue et al. first proposed the environmental friendly reactions between epoxides and CO_2, such as propylene oxide or cyclohexene oxide (CHO), leading to the formation of biodegradable polycarbonates [17,18]. For example, the cyclic alternating copolymerization of CO_2 and propylene oxide yields poly(propylene carbonate) (PPC), a prominent biodegradable polymer of significance in industrial chemistry for their potential to alleviate the greenhouse effect. However, PPC is characterized as the amorphous polymer possessing a low glass transition temperature (T_g) along with compromised

* Corresponding author at: Department of Materials and Optoelectronic Science, Center for Functional Polymers and Supramolecular Materials, National Sun Yat-Sen University, Kaohsiung 80424, Taiwan.
E-mail address: kuosw@faculty.nsysu.edu.tw (S.-W. Kuo).

https://doi.org/10.1016/j.jtice.2023.105214
Received 23 September 2023; Received in revised form 22 October 2023; Accepted 1 November 2023
Available online 16 November 2023

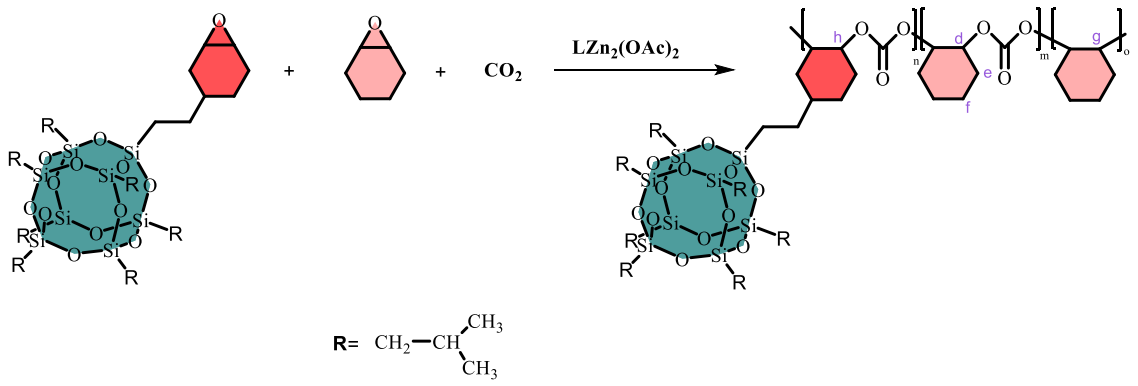

Scheme 1. Synthesis of the PCHCPOSS.

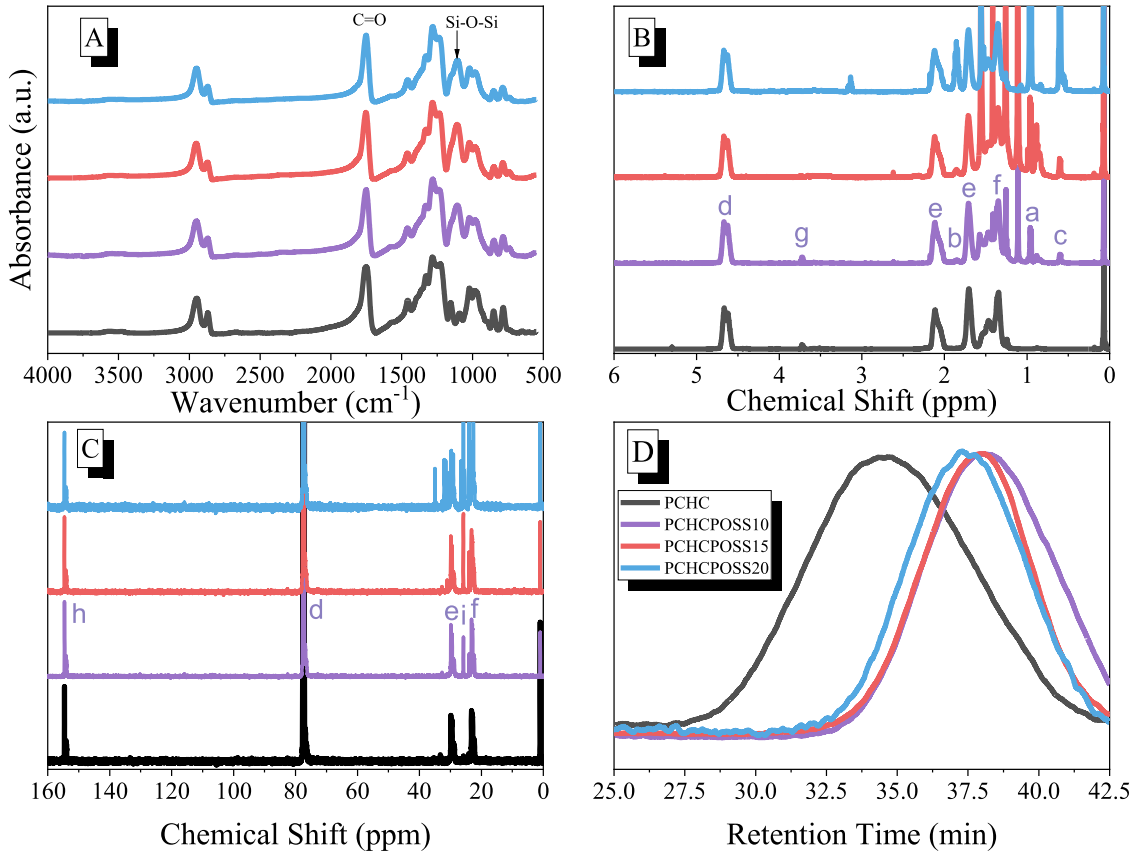

Fig. 1. Synthesis of the PCHCPOSS (A) FTIR, (B) ^{1}H NMR, (C) ^{13}C NMR, (D) GPC spectra.

Table 1
CHO/CHOPOSS/CO_2 polymerization catalyst by $LZn_2(OAc)_2$.[a]

	CHO conv.[b]	POSS (wt %)[c]	PCHC %[d]	M_n (g/mol)	M_w (g/mol)	$Đ$
PCHC	–	–	98.0	24,200	41,100	1.6
PCHCPOSS10	45 %	10	97.9	10,000	14,700	1.4
PCHCPOSS15	35 %	14	96.9	12,000	16,300	1.3
PCHCPOSS20	22 %	16	95.7	12,500	17,600	1.3

[a] Reaction conditions: catalyat:CHO:CHO-POSS = 1:500:X, 20 h, Pco_2 = 346 psi.
[b] Determined by ^{1}H NMR spectrum of the crude product.
[c] Determined by ^{1}H NMR spectrum. POSS(wt%) = $(A_{0.54–0.63}/14) \times 984/(A_{4.3–4.8}/2) \times 142+(A_{0.54–0.63}/14) \times 984 +(A_{3.9–4.0}/2)$.
[d] Determined by ^{1}H NMR spectrum. PCHC = polycarbonate. PCHC% = $(A_{4.3–4.8}/2)/(A_{4.3–4.8}/2 + A_{3.9–4.0}/2)$.

mechanical and thermal stability, which manifests as the inherent brittleness [19–22]. In endeavors to ameliorate its thermal and mechanical characteristics, efforts have been undertaken to augment their molecular weight through copolymerization with alternate monomers such as cyclohexene (CHO) or by blending with other economically viable polymers. For example, we have successfully developed a CO_2 copolymerization process to form poly(cyclohexene carbonate) (PCHC) by ring-opening copolymerization and blending with PVPh through intermolecular hydrogen bonding between C=O units of PCHC and OH units of PVPh, resulting in the formation of miscible PVPh/PCHC binary blends [23].

An alternative approach to enhance the thermal or mechanical properties of polymeric materials involves their incorporation with inorganic materials. A notable illustration is the integration of polyhedral oligomeric silsesquioxane (POSS) nanoparticle into the polymer

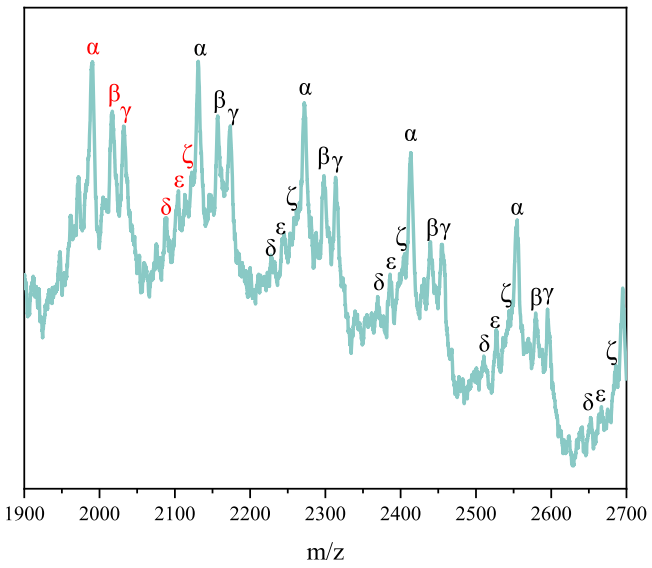

Fig. 2. MALDI-TOF mass of PCHCPOSS20.

main chain or side chain to form the organic/inorganic hybrid materials. POSS has a structure with silica-like core surrounded by eight organic corner groups, and empirical formula is $(RSiO_{1.5})_n$, where R represents an organic group (such as hydrogen, alkyl, alkylene, hydroxyl, or epoxide) [24–29]. The properties of POSS could be effectively modified by different *R* group, making it more widely applications. Indeed, the POSS has excellent properties such as high thermal stability, low flammability, low dielectric constant and low surface energy and copolymerization of POSS nanoparticle could improve the properties of polymers such as surface hardness, mechanical properties, and reduce flammability [30–34].

The influence of POSS nanoparticle as the chain end or side chain in polymeric materials have also been widely discussed in previously studies. For example, the poly(methyl methacrylate) (PMMA) incorporated POSS nanoparticle to form PMMA-*b*-POSS or PMMA-*b*-PMAPOSS block copolymers have been synthesized by using atom transfer radical or anionic polymerization [35]. We have observed the pronounced screening effect for these two kinds of PMMA based POSS block copolymers [36,37]. Specifically, the screening effect, quantified as the γ value, attains 0.65 and 1.0 for PMMA-*b*-POSS and PMMA-*b*-PMAPOSS, respectively, as blending with phenolic or PVPh homopolymer, indicating that the intermolecular hydrogen bonding interaction of C=O units of PMMA was strongly weaken with OH units of PVPh when POSS nanoparticles as side chain or side chain of polymeric materials.

In this study, the isobutyhexyloxide (CHOPOSS) nanoparticle has a ring structure and could be carried out with CHO and CO_2 by ring-opening copolymerization to form PCHCPOSS random copolymers as shown in Scheme 1. The investigation encompassed as in-depth exploration of the synthesis, thermal properties and hydrogen bonding interaction of the pure PCHC, wherein the presence of CHOPOSS cage exerted notable influence. were influenced by the incorporation of CHCPOSS cage was discussed. We believe that the Si-O-Si on the POSS cage will generate forces other than hydrogen bonds (such as dipole-dipole interaction), and POSS will hinder the movement between molecular chains, thus weakening the hydrogen bonding forces within the molecule [38,39]. However, the miscibility, intermolecular hydrogen bonding, and thermal properties of these PCHCPOSS random copolymers with PVPh were characterized through DSC and FTIR analyses. We found that PCHCPOSS cage caused the polymer to produce a screening effect, which becomes more obvious as the POSS content increases. When PCHCPOSS20 was mixed with PVPh, phase separation could be clearly observed from DSC, mainly caused by the screening effect. To our knowledge, this represents the first study of the integration of POSS cage structures into CO_2-based polycarbonates and their hydrogen-bonding interactions with hydroxyl polymers. Prior to this, no one has attempted to synthesize POSS and CO_2 using ring-opening polymerization. Through this study, we can better understand the impact of POSS-containing polymers in blending.

Table 2
MALDI-TOF mass of PCHCPOSS20.

	m/z		structure
α	1990.509	14α	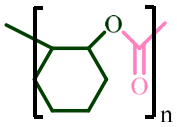
γ	2032.767	14α+CO_2	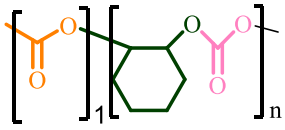
δ	2087.317	14α+CHO	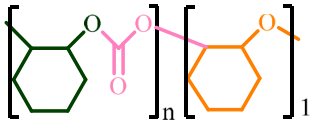
ζ	2122.703	8α+PCHCPOSS	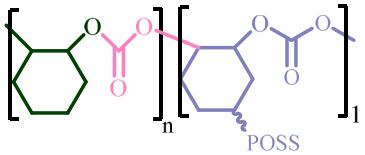

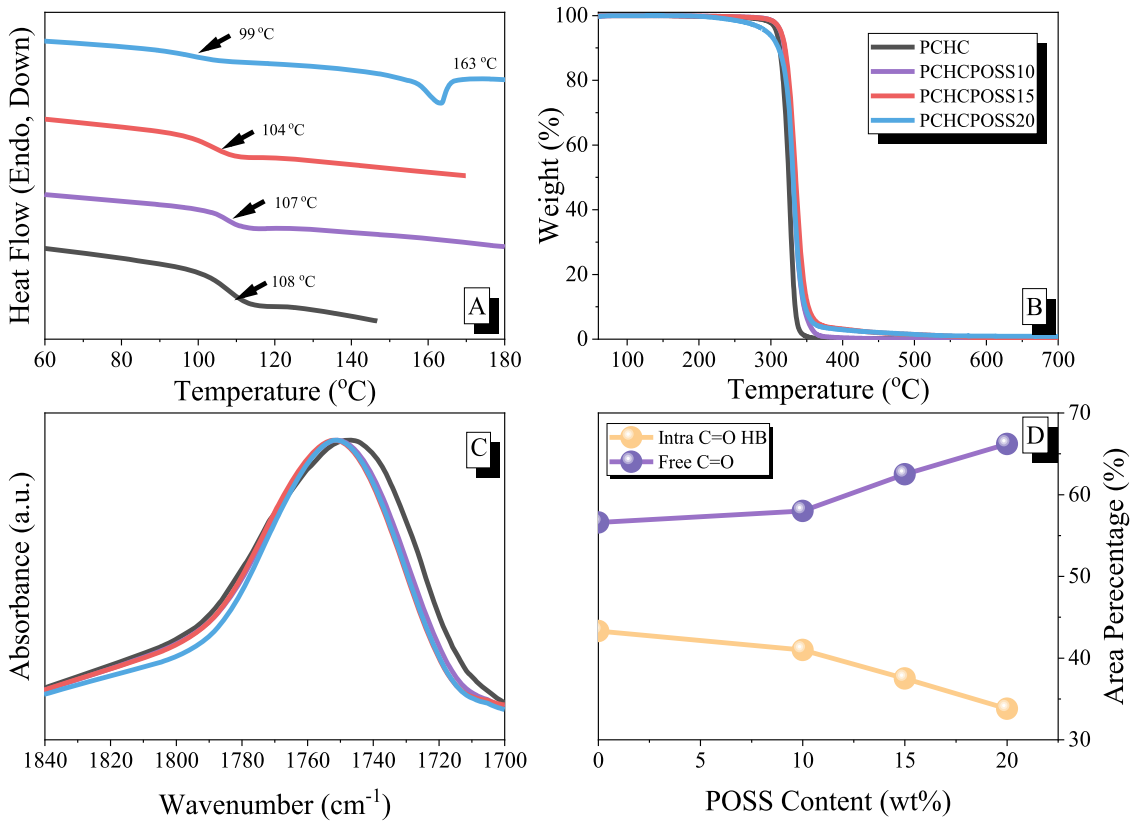

Fig. 3. (A) DSC thermal analyses, (B) TGA thermal analyses; (C) FTIR of C=O group; (D) Area percentage of the free C=O and intramolecularly H-bonded C=O groups in PCHCPOSS.

2. Experimental section

2.1. Materials

All solvents and reagents were used in their as-received, unless otherwise mentioned. The materials included *o*-Vanillin (99 %), 2,2-dimethyl-1,3-propanediamine (99 %), cyclohexene oxide (CHO), dichloromethane (DCM), tetrahydrofuran (THF), all purchased from Acros Organic. Prior to use, CHO was refluxed over calcium hydride (CaH_2) for 24 h and vacuum distilled. The epoxycyclohexyl isobutyl POSS (CHOPOSS) was sourced from Kingpak Technology Inc., and used without any additional purification steps. Zinc acetate dihydrate (98 %) was obtained from SHOWA, and high purity CO_2 (> 99.999 %) was obtained from the Hsin E-Li Gas Industrial Co., Ltd. Zinc catalyst ($LZn_2(OAc)_2$) was synthesized and analyzed in previous study [23].

2.2. Copolymerization of CO_2, CHO and CHOPOSS

A quantity of zinc catalyst ($LZn_2(OAc)_2$ 0.0976 g) was combined with various amounts of epoxycyclohexyl isobutyl POSS (10, 15, and 20 wt%) into the autoclave with a magnetic stirring bar. The autoclave, equipped with a vacuum line, was subsequently connected to the reaction system. To avoid moisture, the autoclave containing the catalyst inside was further dried under vacuum at 100 °C for 8 h. Following the cooling stage, the autoclave was purged with CO_2 and 8 mL CHO was introduced to the autoclave. The ensuing copolymerization was maintained in an oil-bath with 80 °C for 20 h under the consistent CO_2 pressure of 435 psi. Then, the reactor was allowed to cool, and the unreacted CO_2 was carefully released. Those resultant mixtures were dissolved in DCM and extracted with a 5 % dilute hydrochloric acid solution. The final PCHC-*co*-PCHCPOSS product was multiple precipitated in THF/Deionized water (DI water) mixture, followed by drying in a vacuum oven at 60 °C. Notably, the nomenclature was used to PCHC-*co*-PCHCPOSS based on their distinct POSS composition, referred to as PCHCPOSS10, PCHCPOSS15 and PCHCPOSS20, respectively. ^{1}H NMR (500 MHz, $CDCl_3$, δ, ppm): 4.6 (Cy**C**HOCO$_2$), 3.5 (Cy**C**HOC), 1.26–2.26 (Cy**C**H$_2$), 1.85 (Si-CH$_2$—C**H**-(CH$_3$)$_2$), 0.96 (Si-CH$_2$—CH-(C**H**$_3$)$_2$), 0.6 (Si-C**H**$_2$—CH-(CH$_3$)$_2$). ^{13}C NMR (125 MHz, $CDCl_3$, δ, ppm): 154.4 (C=O), 76.7 (Cy**C**HOCO$_2$), 21.9–30.7 (Cy**C**H$_2$), 32.6 (Si-**C**H$_2$—CH-(CH$_3$)$_2$). FTIR (KBr, cm^{-1}): 1750 (C=O).

2.3. Binary blends of PVPh/PCHCPOSS

Different binary PVPh/PCHCPOSS blends were meticulously crafted by a THF solution-casting with 5 wt% mixtures were subjected to stirring for 24 h. The THF solvent was allowed to undergo gradually evaporated over a span of 7 days at room temperature and the residual THF solvent was slowly removed under a high vacuum condition at 40 °C for 5 days.

3. Result and discussion

3.1. Synthesis of PCHCPOSS random copolymers

The PCHCPOSS random copolymers were been synthesized by ring opening copolymerization of carbon dioxide as shown in Scheme 1 and comprehensive characterized by FTIR, ^{1}H, ^{13}C NMR, and GPC analyses. Fig. 1(A) shows the FTIR spectra of various PCHCPOSS random co-polymers. Firstly, the absorptions at 2950 and 2870 cm^{-1} were corresponding to aliphatic CH, CH$_2$ and CH$_3$ groups vibration, the strong absorbance peaks of C=O were observed at 1750 cm^{-1}, suggesting successfully synthesis of linear carbonate instead of cyclic carbonate as expected [40,41]. The most importantly, it could be found that the strong absorbance peak of Si-O-Si at 1100 cm^{-1}, indicating the existence of POSS cage in PCHCPOSS copolymers. Fig. 1(B) presents their

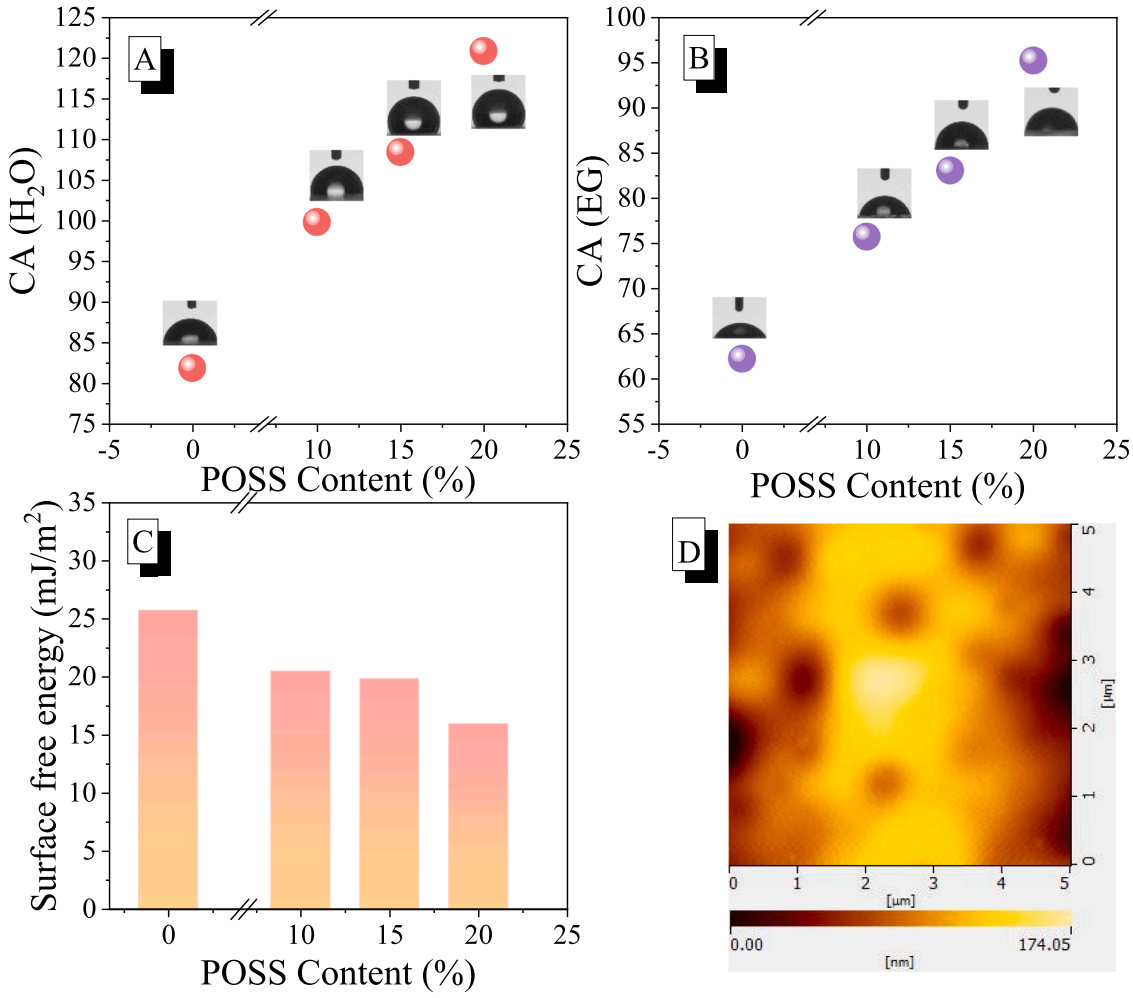

Fig. 4. Interaction of a solvent droplet with PCHCPOSS: (A) H_2O, and (B) EG; (C) Surface energy; (D) AFM image of pure PCHCPOSS10.

corresponding ^{1}H NMR spectra of the PCHCPOSS random copolymers. This terpolymer was synthesized using CHO, CO_2, and CHOPOSS as the monomers. Therefore, the spectrum illustrates the chemical composition and structural characteristics resulting from the copolymerization. The signals at 0.6, 0.96 and 1.85 ppm represent Si-C**H**$_2$–CH-(CH$_3$)$_2$, Si-CH$_2$–CH-(C**H**$_3$)$_2$ and Si-CH$_2$–C**H**-(CH$_3$)$_2$ of isobutyl POSS, respectively. Then, the signals of cyclohexyl CH$_2$ on the side chain of CHOPOSS unit were located at 1.34, 1.70 and 2.11 ppm. Furthermore, the signal of cyclohexyl CH on the main chain was observed at 4.6 ppm. The PCHCPOSS content can be calculated by the integrating signals, the PCHCPOSS content of PCHCPOSS10, PCHCPOSS15 and PCHCPOSS20 were 10, 14 and 16 wt%, respectively, and were summarized in Table 1. Therefore,the polyether content was within 5 %, and more than 95 % consisted of linear polycarbonate. Moreover, the high content of POSS resulted in a decrease in the conversion of CHO, mainly attributed to the bulky moiety of POSS cage structure. The steric hindrance of POSS made it difficult for CHOPOSS react with CO_2 and CHO, as shown in Fig. S1.

In the ^{13}C NMR spectra as Fig. 1(C), the chemical shift of the Si-CH$_2$–CH-(**C**H$_3$)$_2$ and Si-**C**H$_2$–CH-(CH$_3$)$_2$ signal in isobutyl POSS was observed at 32.66 and 32.68 ppm, respectively. The cyclohexyl CH signal on the main chain appeared at 76.87 ppm, and the cyclohexyl CH$_2$ signals on the side chain of CHOPOSS were observed at 23.18 and 29.84 ppm, respectively. Additionally, the carbon signal of C=O was detected at 154.4 ppm, indicating the presence of carbonate group in the PCHCPOSS copolymer unit and confirming the successful copolymerization of carbon dioxide with the monomer. Fig. S2 displays the ^{29}Si NMR spectra of the PCHCPOSS random copolymers. The peaks at −21.4 and −66.37 ppm were corresponding to O**Si**CH$_2$CH(CH$_3$)$_2$ and Si-O-**Si**-O cage units, indicating that CHOPOSS monomer had been successfully synthesized with CHO and CO_2. The molecular weights of the PCHCPOSS random copolymers were determined through GPC analyses, as illustrated in Fig. 1(D). Upon the addition of PCHCPOSS, a significant decrease in the molecular weight was observed. This decrease can be attributed to the presence of the bulky POSS group, which is likely reduced the reactivity of the monomers, consequently leading to the formation of polymers with lower molecular weights. However, as the content of POSS was increased to 20 wt%, the molecular weight was beginning to increase due to the significantly higher molecular weight of CHOPOSS unit in comparison to the CHO unit. Furthermore, it was possible that the polymer contains POSS structure, which might result in POSS exerting interaction with GPC column, thereby leading to a reduced measured molecular weight.

To understand the composition and structure of PCHCPOSS random copolymers, the results of MALDI-TOF mass were presented in Fig. 2 and Fig. S3. The difference between the peaks at 1990.509 *m/z* (α) and 2132.945 *m/z* (α) is approximately 142 g/mol, which was equal to the summed molecular weight (M_w) of one carbon dioxide and one cyclohexene oxide unit. Then, the 1990.509 *m/z* (α) corresponding to 14 cyclohexene carbonate units. Similarly, the difference between 1990.509 *m/z* (α) and 2032.767 *m/z* (γ) was ca. 44 g/mol, which precisely matches the molecular weight of one carbon dioxide unit. Furthermore, the difference between 2087.317 *m/z* (δ) and 1990.509 *m/z* (α) was ca. 98 g/mol, representing one cyclohexene oxide unit. Moreover, the peak at 2104.797 *m/z* (ε) exhibits one oxygen atom at the

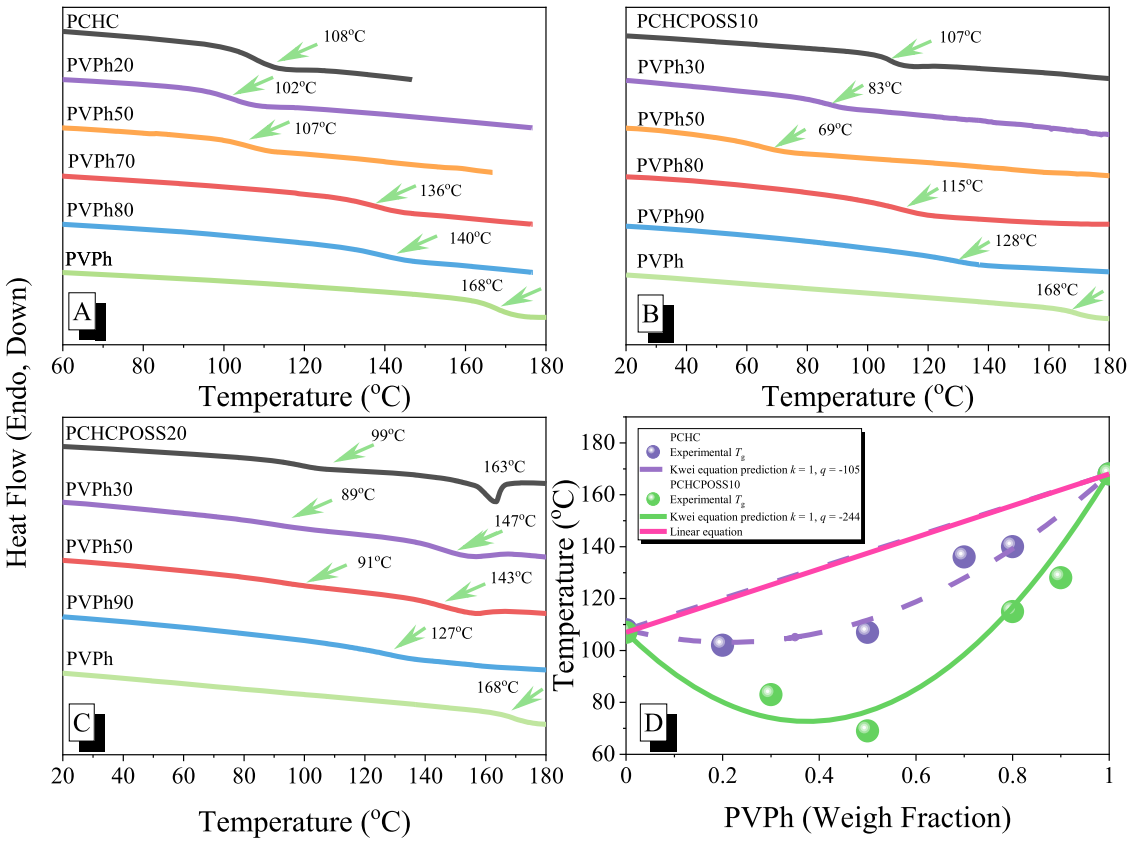

Fig. 5. (A-C) DSC thermal analyses: (A) PCHC/PVPh, (B) PCHCPOSS10/PVPh, (C) PCHCPOSS20/PVPh; (D) Corresponding values of T_g predicted by the linear rule and the Kwei equation.

end of the copolymer compared to the 2087.317 *m/z* (δ). Regarding the peak at 2016.962 *m/z* (β), in comparison to the 1990.509 *m/z* (α), it had one more carbon dioxide unit, one less cyclohexene carbonate unit, and one less oxygen atom in the cyclohexene carbonate unit. Lastly, the 2122.703 *m/z* (ζ) corresponds to 8 units of PCHC with an additional PCHCPOSS unit. These discernible mass differences provide as valuable insights into the composition and arrangement of PCHCPOSS random copolymers (Table 2).

Fig. 3(A) shows the thermal analysis for both pure PCHC and PCHCPOSS copolymers with different CHCPOSS contents. After-introducing the CHCPOSS units into the random copolymers, T_g values has a slightly drop from 108 to 107, 104 and 99 °C with CHCPOSS units increasing, because the bulky POSS group as the side chain may increase the free volume of the whole system, and produce a dilution effect, which weakens the dipole-dipole interaction and intramolecular hydrogen bonds of pure PCHC. Furthermore, PCHCPOSS20 displays the melting point, probably due to the aggregation of POSS cage structure [42–44]. The thermal stability of these PCHCPOSS copolymers were also measured by TGA analyses as shown in Fig. 3(B). The thermal degradation temperature (T_{d10}) and char yield exhibited an upward trend upon increasing CHOPOSS compositions in PCHCPOSS random copolymers from 312 °C for pure PCHC (0 wt% for char yield) to 319 °C for PCHCPOSS10, 324 °C for PCHCPOSS15 and 325 °C (3.4 wt% for char yield) for PCHCPOSS20, aligning with expectations. The incorporation of inorganic POSS unit could provide better thermal stability due to the limitation of volatility to produce the ceramic residue with high char yield during heating in nitrogen atmosphere.

To understand the influence of POSS cage on the thermal properties of PCHCPOSS random copolymer, the expanded FTIR spectra from Fig. 1 (A) was summarized in Fig. 3(C). After adding CHCPOSS into the PCHC copolymers, the half width at half maximum was decreased as the increase of POSS cage contents, which leads to the intramolecular H-bonding interaction slightly decreased. As mentioned in previous study [20], two major absorptions due to the free C=O and intramolecular H-bonding C=O units [C=O···H—C] in six-membered ring at 1763 cm^{-1} and 1735 cm^{-1}, respectively, which is similarly reported in the PLA main chain. In order to identify the interaction between the free C=O and intramolecular H-bonding C=O of PCHCPOSS copolymers Fig. S4 displays 1700–1800 cm^{-1} region from C=O of PCHCPOSS and curve fitting of the spectra of PCHCPOSS copolymers as shown in Fig. 3(D). When content of CHCPOSS units was increased, the intramolecular H-bonding C=O signal was decreased, indicating that the T_g may have a slightly drop from 108 to 99 °C when the incorporation of CHOPOSS in the random copolymers.

Furthermore, the PCHCPOSS should possess good hydrophobicity and the surface properties by changing the amounts of CHCPOSS units in PCHCPOSS random copolymer through the contact angle measurement as shown in Fig. 4. The water contact angle of pure PCHC is 81.8°, which belongs to hydrophilicity. However, as the amounts of CHOPOSS compositions were increased in PCHCPOSS random copolymers, the water contact angles of PCHCPOSS were increased. The contact angles were 99.8°, 108.4° and 120.8° for PCHCPOSS10, PCHCPOSS15 and PCHCPOSS20, respectively. PCHCPOSS was transformed to the hydrophobic materials.

Figs. 4(D) and S5 depict atomic force microscopy (AFM) images of PCHCPOSS rotating on a glass substrate. In the AFM image of the pure PCHC film, the film surface appeared smooth, exhibiting a root mean-square (rms) roughness of 3.2 nm. Upon the addition of POSS, the surface roughness exhibited a gradual increase, with the rms value from 9.6 to 17.1 nm. When the POSS content is too less, it becomes too diluted within the random copolymer, and the aggregation does not occur. However, as the POSS content increases, such as PCHCPOSS20, it becomes evident that POSS particles start to aggregate, leading to a noticeable roughening of the surface, as illustrated in Fig. S5. This

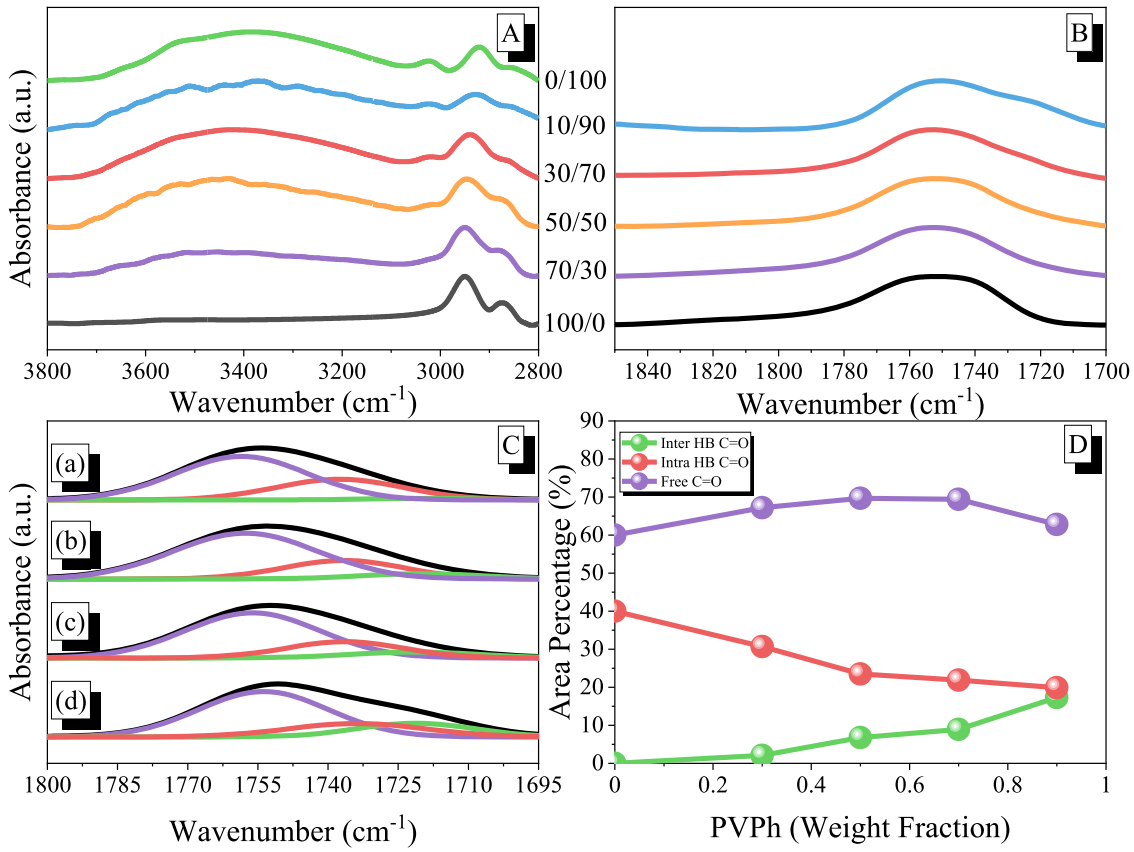

Fig. 6. FTIR spectra of the various PCHCPOSS10/PVPh binary blend, recorded at 120 °C: (A) OH, and (B) C=O region; (C): (a-d) Curve fitting of the C=O absorptions of selected PCHCPOSS10 (a) PVPh30, (b) PVPh50, (c) PVPh70, (d) PVPh90; (D) Area fraction of the free C=O, intermolecularly H-bonded C=O and intramolecularly H-bonded C=O groups in PCHCPOSS10/PVPh binary blend.

outcome aligned with the findings from contact angle. Notably, PCHC is inherently hydrophilic. Nevertheless, with the incorporation of POSS, the film surface began to display increased roughness, leading to enhanced hydrophobicity in PCHCPOSS.

3.2. Analyses of PCHCPOSS/PVPh binary blends

Fig. 5 shows the DSC thermal analysis of pure PCHC, PCHCPOSS copolymers, pure PVPh, and their corresponding binary blends. The binary blend of PCHC/PVPh exhibits single T_g at any composition ratio as shown in Fig. 5(A), indicating completely miscibility between them, as mentioned in previous study [23]. Upon the addition of CHCPOSS units into PCHCPOSS copolymers, we could observe that the PVPh/PCHCPOSS10 binary blends also exhibit single T_g values in Fig. 5 (B). However, two distinct T_g values were observed in PVPh/PCHCPOSS20 binary blends as shown in Fig. 5(C), indicating partially miscible or immiscible behavior in this binary blend. Clearly, the incorporation of CHCPOSS units into the PCHCPOSS random copolymers strongly affect the miscibility behavior with PVPh homopolymer. Firstly, we applied the Kwei equation to explain the PVPh/PCHCPOSS binary blends, as shown in Fig. 4(D) and as follows [45]:

$$T_g = \frac{W_1 T_{g1} + kW_2 T_{g2}}{W_1 + kW_2} + qW_1 W_2$$

where W_1 or W_2 is weight fraction of each polymer, T_{g1} or T_{g2} is each glass transition temperature of PCHCPOSS or PVPh, and k and q are the fitting constant. The q value is strongly dependent on the intermolecular hydrogen bonding strength of binary polymer blends. In our previous study, we extensively discussed the hydrogen bonding interactions between PVPh/PCHC binary blends and it exhibited the $k = 1$, $q = -105$ based on the Kwei equation as shown in Fig. 5(D), indicating that average intermolecular H-bonding strength (OH···O=C) in PVPh/PCHC blends is weaker than the self-association H-bonding strength (OH···OH) of pure PVPh. Upon the addition of CHOPOSS cage into PCHCPOSS random copolymer, the PVPh/PCHCPOSS10 binary blend displayed the $k = 1$, $q = -245$ based on the Kwei equation as also displayed in Fig. 5 (D), which is much stronger negative deviation compared with PVPh/PCHC binary blend, also indicating much weaker intermolecular H-bonding interactions in the PCHCPOSS10/PVPh blend than self-association H-bonding interaction of the pure PVPh. As mentioned previously [46], the POSS cage at the side chain in carbonyl based polymer such as PMMA would have strong screening effect to inhibit the intermolecular hydrogen bonding interaction between C=O group and OH group. As a result, PCHCPOSS10 random copolymer also displayed the limitation of intermolecular H-bonding between —C=O group of PCHC and OH group of PVPh. Further increasing CHCPOSS units into PCHCPOSS20 random copolymer, the PVPh/PCHCPOSS20 binary blend even displayed two T_g values, indicating partially miscible or immiscible. Therefore, the intermolecular H-bonding interaction between C=O group and OH group becomes much weaker.

Figs. 6 and 7 show the FTIR spectra of binary PVPh/PCHCPOSS10 and PVPh/PCHCPOSS20 blends that measured at 120 °C to avoid moisture absorption, respectively. Figs. 6(A) and 7(A) represent the OH stretching absorption in the range of 3100–3600 cm^{-1}, which include the characteristic absorption of free OH groups at 3540 cm^{-1}, as well as the indicative absorption related to the self-association of OH···OH interactions at 3385 cm^{-1} for pure PVPh. When the PCHCPOSS10 or PCHCPOSS20 content increases, the intensity of free OH group was increased and the self-association OH group was shifted to higher wavenumber at ca. 3445 cm^{-1}, indicating that the intermolecular

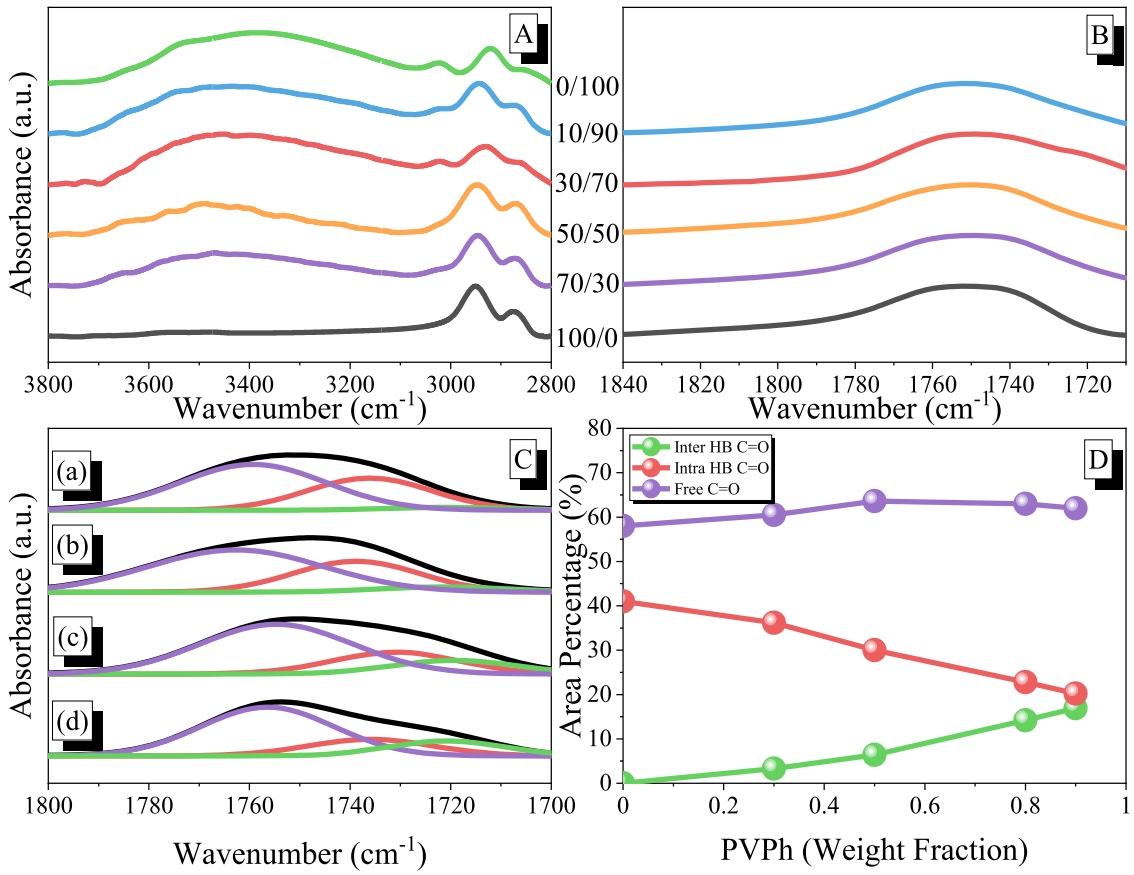

Fig. 7. FTIR spectra of the various PCHCPOSS20/PVPh binary blend, recorded at 120 °C: (A) OH, and (B) C=O region; (C): (a-d) Curve fitting of the C=O absorptions of selected PCHCPOSS10 (a) PVPh30, (b) PVPh50, (c) PVPh70, (d) PVPh90; (D) Area fraction of the free C=O, intermolecularly H-bonded C=O and intramolecularly H-bonded C=O groups in PCHCPOSS20/PVPh binary blend.

OH···O=C H-bonding interaction strength of PVPh/PCHCPOSS is weaker than the self-association OH···OH H-bonding interaction of pure PVPh [47]. This result is consistent with Kwei equation where the q was exhibited the negative value. Furthermore, their corresponding FTIR spectra of C=O stretching at 120 °C as shown in Figs. 6(B) and 7(B).

According to the previous research [18], the C=O group of PCHCPOSS in PVPh/PCHCPOSS binary blends could be composed into three parts: free C=O at 1760 cm^{-1}, intramolecular C=O from PCHCPOSS unit at 1735 cm^{-1}, and additionally, a peak appears for the C=O group, indicating the formation of intermolecular H-bonding between the C=O group of PCHCPOSS unit and the OH group of PVPh at 1720 cm^{-1}. In order to understand the areapercentage of each absorption, Figs. 6(C) and 7(C) exhibit the curve fitting of the C=O group of PVPh/PCHCPOSS10 and PVPh/PCHCPOSS20 binary blends with different compositions. In addition, the areapercentage of free C=O unit, intramolecular hydrogen bonded C=O from PCHCPOSS unit and intermolecular H-bonded C=O with PVPh were summarized in Figs. 6(D) and 7(D).

Clearly, the areapercentage of intramolecular H-bonded of C=O from PCHPCPOSS were both decreased; however, the areapercentages of intermolecular hydrogen boned C=O with PVPh were increased with the increase of PVPh concentrations in all binary blends. Furthermore, the areapercentage of intermolecular H-bonded C=O with PVPh was decreased with the increase of POSS concentrations due to the screening effect by the addition of POSS cage structure as mentioned in previous work [35] as expected.

4. Conclusions

We have successfully synthesized various POSS compositions within PCHCPOSS random copolymers through the process of ring-opening copolymerization and prepared a series of binary PVPh/PCHCPOSS blends, followed by DSC and FTIR analyses. The binary blend of PVPh/PCHCPOSS10 exhibited single T_g values behavior at entire compositions, indicating completely miscibility; however, this binary blend displayed strongly negative q value based on the Kwei equation and even was lower than that observed in the PVPh/PCHC binary blend that lacked the POSS component. As a result, as the concentration of POSS cage was increased in PVPh/PCHCPOSS20 binary blends, which showed two distinct T_g values, representing towards microphase separation, particularly evident at relatively lower PVPh concentrations. This microphase separation phenomenon is primarily attributed to the screening effect induced by the presence of POSS in PVPh/PCHCPOSS blends, leading to a reduction in intermolecular hydrogen bonds. Overall, this work provides the fundamental insights into the POSS cage structure within PCHC random copolymers and elucidates the intricate interplay of the compete H-bonding interaction in PVPh/PCHCPOSS binary blends.

Declaration of Competing Interest

The authors declare that they have no known competing financial interests or personal relationships that could have appeared to influence the work reported in this paper.

Acknowledgments

This study was supported financially by the National Science and Technology Council, Taiwan, under contracts NSTC 112–2218-E-110–007 and 112–2223-E-110–002. The authors thank National Sun

Yat-sen University staff for their assistance with the TEM (ID: EM022600) experiments.

Supplementary materials

Supplementary material associated with this article can be found, in the online version, at doi:10.1016/j.jtice.2023.105214.

References

[1] Peter SC. Reduction of CO_2 to chemicals and fuels: a solution to global warming and energy crisis. ACS Energy Lett 2018;3:1557–61.
[2] Bera R, Ansari M, Alam A, Das N. Triptycene, phenolic-OH, and azo-functionalized porous organic polymers: efficient and selective CO_2 capture. ACS Appl Polym Mater 2019;1:959–68.
[3] Tackett BM, Gomez E, Chen JG. Net reduction of CO_2 via its thermos catalytic and electrocatalytic transformation reactions in standard and hybrid processes. Nat Catal 2019;2:381–6.
[4] Mohamed MG, Elewa AM, Li MS, Kuo SW. Construction and multifunctional of hypercrosslinked porous organic polymers containing ferrocene unit for high-performance iodine adsorption and supercapacitor. J Taiwan Inst Chem Eng 2023;150:105045.
[5] Allen SD, Moore DR, Lobkovsky EB, Coates GW. High-activity, single-site catalysts for the alternating copolymerization of CO_2 and propylene oxide. J Am Chem Soc 2002;124:14284–5.
[6] Mousa AO, Mohamed MG, Chuang CH, Kuo SW. Carbonized aminal-linked porous organic polymers containing Pyrene and Triazine units for gas uptake and energy storage. Polymers 2023;15:1891 (Basel).
[7] Cao PZ, Wang Z, Liu LY, Gao P, Tian G, Liu HR, He JX. Synthesis of cobalt-silicon molecular sieve with excellent CO_2/N_2 adsorption selectivity for dynamic CO_2 capture. J Taiwan Inst Chem Eng 2022;138:104444.
[8] Samy MM, Mohamed MG, Mansoure TH, Meng TS, Khan MAR, Liaw CC, Kuo SW. Solid state chemical transformations through ring-opening polymerization of ferrocene-based conjugated microporous polymers in host-guest complexes with benzoxazine-linked cyclodextrin. J Taiwan Inst Chem Eng 2022;132:104110.
[9] Ejaz M, Mohamed MG, Kuo SW. Solid state chemical transformation provides a fully benzoxazine-linked porous organic polymer displaying enhanced CO_2 capture and supercapacitor performance. Polym Chem 2023;14:2494–509.
[10] Mohamed MG, Chang SY, Ejaz M, Samy MM, Mousa AO, Kuo SW. Design and synthesis of bisulfone-linked two-dimensional conjugated microporous polymers for CO_2 adsorption and energy storage. Molecules 2023;28:3234.
[11] Mohamed MG, Chen TC, Kuo SW. Solid-state chemical transformations to enhance gas capture in benzoxazine-linked conjugated microporous polymers. Macromolecules 2021;54:5866–77.
[12] Mohamed MG, Sharma SU, Liu NY, Mansoure TH, Samy MM, Chaganti SV, Chang YL, Lee JT, Kuo SW. Ultrastable covalent triazine organic framework based on anthracene moiety as platform for high-performance carbon dioxide adsorption and supercapacitors. Int J Mol Sci 2022;23:3174.
[13] Mohamed MG, Ahmed MMM, Du WT, Kuo SW. Meso/microporous carbons from conjugated hyper-crosslinked polymers based on tetraphenylethene for high-performance CO_2 capture and supercapacitor. Molecules 2021;26:738.
[14] Leung DYC, Caramanna G, Maroto-Valer MM. An overview of current status of carbon dioxide capture and storage technologies. Renew Sust Energ Rev 2014;39:426–43.
[15] Jiang X, Nie X, Guo X, Song C, Chen JG. Recent advances in carbon dioxide hydrogenation to methanol via heterogeneous catalysis. Chem Rev 2020;120:7984–8034.
[16] Hill MR, Tang S, Masada K, Hirooka Y, Nozaki K. Incorporation of CO_2-derived bicyclic lactone into conventional vinyl polymers. Macromolecules 2022;55:3311–6.
[17] Inoue S, Koinuma H, Tsuruta T. Copolymerization of carbon dioxide and epoxide. J Polym Sci Polym Lett 1969;7:287–92.
[18] Inoue S, Koinuma H, Tsuruta T. Copolymerization of carbon dioxide and epoxide with organometallic compounds. Makromol Chem 1969;130:210–20.
[19] Li Y, Shimizu H. Compatibilization by homopolymer: significant improvements in the modulus and tensile strength of PPC/PMMA blends by the addition of a small amount of PVAc. ACS Appl Mater Interface 2009;1:1650–5.
[20] Meereboer KW, Pal AK, Misra M, Mohanty AK. Green composites from a bioplastic blend of poly(3-hyroxybutyrate-*co*-3-hydroxyvalerate) and carbon dioxide-derived poly(propylene carbonate) and filled with a corn ethanol-industry co-product. ACS Omega 2021;6:20103–11.
[21] Song L, Li Y, Meng X, Wang T, Shi Y, Wang Y, Shi S, Liu LZ. Crystallization, structure and significantly improved mechanical properties of PLA/PPC blends compatibilized with PLA-PPC copolymers produced by reactions initiated with TBT or TDI. Polymers 2021;13:3245 (Basel).
[22] Yu T, Zhou Y, Zhao Y, Liu KP, Chen EQ, Wang DJ, Wang FS. Hydrogen-bonded thermostable liquid crystalline complex formed by biodegradable polymer and amphiphilic molecules. Macromolecules 2008;41:3175–80.
[23] Du WT, Kuan YL, Kuo SW. Intra- and intermolecular hydrogen bonding in miscible blends of CO_2/epoxy cyclohexene copolymer with poly(vinyl phenol). Int J Mol Sci 2022;42:7018.
[24] Shao Y, Ding M, Xu Y, Zhao F, Dai H, Miao XR, Yang S, Li H. Synthesis and self-assembly of shape amphiphiles based on POSS-dendron conjugates. Molecules 2017;22:622.
[25] Mohamed MG, Kuo SW. Progress in the self-assembly of organic/inorganic polyhedral oligomeric silsesquioxane (POSS) hybrids. Soft Matter 2022;18:5535–61.
[26] Fan L, Wang X, Wu D. Polyhedral oligomeric silsesquioxanes (POSS)-based hybrid materials: molecular design, solution self-assembly and biomedical applications. Chin J Chem 2021;39:757–74.
[27] Mohamed MG, Tsai MY, Wang CF, Huang CF, Danko M, Dai L, Chen T, Kuo SW. Multifunctional polyhedral oligomeric silsesquioxane (POSS) based hybrid porous materials for CO_2 uptake and iodine adsorption. Polymers 2021;13:221 (Basel).
[28] Mohamed MG, Liu NY, El-Mahdy AFM, Kuo SW. Ultrastable luminescent hybrid microporous polymers based on polyhedral oligomeric silsesquioxane for CO_2 uptake and metal ion sensing. Microporous Mesoporous Mater 2021;311:110695.
[29] Chen WC, Tsao YH, Wang CF, Huang CF, Dai L, Chen T, Kuo SW. Main chain–type block copolymers through atom transfer radical polymerization from double-decker–shaped polyhedral oligomeric silsesquioxane hybrids. Polymer 2020;12:465 (Guildf).
[30] Liu T, Zhao H, Li J, Zhang D, Zheng W, Wang L. POSS-tetraaniline based giant molecule: synthesis, self-assembly, and active corrosion protection of epoxy-based organic coatings. Corros Sci 2020;168:108555.
[31] Wang YK, Tsai FC, Ma CC, Wang ML, Kuo SW. Using methacryl-polyhedral oligomeric silsesquioxane as the thermal stabilizer and plasticizer in poly(vinyl chloride) nanocomposites. Polymers 2019;11:1711 (Basel).
[32] Mohamed MG, Kuo SW. Functional polyimide/polyhedral oligomeric silsesquioxane nanocomposites. Polymers 2019;11:26 (Basel).
[33] Zou H, Li QW, Wu QL, Liang WQ, Hou XH, Zhou L, Liu N, Wu ZQ. POSS-based starlike hybrid helical poly(phenyl isocyanide)s: their synthesis, self-assembly, and enantioselective crystallization ability. Polym Chem 2021;12:3917–24.
[34] Zhao B, Mei H, Wang H, Li L, Zhen S. Organic–inorganic polyureas with POSS cages in the main chains via polycondensation of diamines with carbon dioxide. ACS Appl Polym Mater 2022;4:509–20.
[35] Huang CF, Kuo SW, Lin FJ, Huang WJ, Wang CF, Chen WY, Chang FC. Influence of PMMA-chain-end tethered polyhedral oligomeric silsesquioxanes on the miscibility and specific interaction with phenolic blends. Macromolecules 2006;39:30008.
[36] Chen WC, Lin RC, Tseng SM, Kuo SW. Minimizing the strong screening effect of polyhedral oligomeric silsesquioxane nanoparticles in hydrogen-bonded random copolymers. Polymers 2018;10:303 (Basel).
[37] Chiou CW, Lin YC, Wang L, Hirano C, Suzuki Y, Hayakawa T, Kuo SW. Strong screening effect of polyhedral oligomeric silsesquioxanes (POSS) nanoparticles on hydrogen bonded polymer blends. Polymers 2014;6:926–48 (Basel).
[38] Kuo SW. Hydrogen bonding interactions in polymer/polyhedral oligomeric silsesquioxane nanomaterials. J Polym Res 2022;29:69.
[39] Lee YJ, Kuo SW, Huang WJ, Lee HY, Chang FC. Miscibility, specific interactions, and self-assembly behavior of phenolic/polyhedral oligomeric silsesquioxane hybrids. J Polym Sci Part B Polym Phys 2004;42:1127–36.
[40] Thevenon A, Garden JA, White AJP, Williams CK. Dinuclear zinc salen catalysts for the ring opening copolymerization of epoxides and carbon dioxide or anhydrides. Inorg Chem 2015;54:11906–15.
[41] Zhang YY, Yang GW, Wang Y, Lu XY, Wu GP, Zhang ZS, Wang K, Zhang RY, Nealey PF, Darensbourg DJ, Xu ZK. Synthesis of CO_2-based block copolymers via chain transfer polymerization using macroinitiators: activity, blocking efficiency, and nanostructure. Macromolecules 2018;51:791–800.
[42] Zhang Y, Lee S, Yoonessi M, Liang K, Pittman CU. Phenolic resin− trisilanolphenyl polyhedral oligomeric silsesquioxane (POSS) hybrid nanocomposites: morphology and structure. Polymer 2006;47:2984–96 (Guildf).
[43] Strachota A, Kroutilová I, Kovářová J, Matějka I. Epoxy networks reinforced with polyhedral oligomeric silsesquioxanes (POSS). thermomechanical properties. Macromolecules 2004;37:9457–64.
[44] Fina A, Monticelli O, Camino G. POSS-based hybrids by melt/reactive blending. J Mater Chem 2010;20:9297–305.
[45] Kwei TK. The effect of hydrogen bonding on the glass transition temperatures of polymer mixtures. J Polym Sci Polym Lett Ed 1984;22:307–13.
[46] Huang CF, Kuo SW, Lin FJ, Huang WJ, Wang CF, Chen WY, Chang FC. Influence of PMMA-chain-end tethered polyhedral oligomeric silsesquioxanes on the miscibility and specific interaction with phenolic blends. Macromolecules 2006;39:300–8.
[47] Kuo SW. Hydrogen bonding in polymeric materials. Hoboken NJ USA: John Wiley & Sons; 2018.